XL CILAMCE
IBERO-LATIN AMERICAN CONGRESS ON COMPUTATIONAL METHODS IN ENGINEERING
NOVEMBER 11-14, 2019
Praiamar Natal Hotel & Convention
Natal, RN-BRAZIL

A STUDY ON EFFECTIVE THERMAL CONDUCTIVITIES OF PERIODIC COMPOSITES REINFORCED BY UNIDIRECTIONAL LONG FIBERS

Eduardo N. Lages
enl@ctec.ufal.br
Laboratory of Scientific Computing and Visualization, Center of Technology, Federal University of Alagoas
Campus A. C. Simões, 57072-900, Maceió, Alagoas, Brasil
Severino P. C. Marques
smarques@ctec.ufal.br
Laboratory of Scientific Computing and Visualization, Center of Technology, Federal University of Alagoas
Campus A. C. Simões, 57072-900, Maceió, Alagoas, Brasil.

Abstract. Due to their excellent physical properties, the composite materials have achieved an increasing field of industrial applications over the last decades. In many of these applications such materials are subjected to high thermal gradients which can generate critical stresses and strains. The magnitude and distribution of the thermal fields induced inside a device or structural element have strong dependency on the composite microstructure. For the analysis and design of these composite systems under thermomechanical loading, the effective thermal conductivity of the material is a property of paramount importance. This effective property depends on many microstructural details, such as, volume fractions and thermal conductivities of the constituent phases, geometrical shapes and distribution of the fibers, among others. The present work consists in a theoretical investigation on the influences of the cross section geometry and volume fraction of the fibers and the contrast between thermal conductivities of the phases of unidirectional periodic fiber reinforced composites. To develop the study, a semi-analytical model expressed in terms of Fourier series and based on the thermal equivalent inclusion strategy is employed. Those mentioned influences are illustrated and discussed for several numerical examples. Results obtained by other homogenization procedures available in the literature are also presented to demonstrate the efficiency of the model used in the study.

Keywords: Periodic composites, Thermal conductivity, Fiber influence, Semi-analytical model

1 Introduction

Due to their unique properties, the composite materials have achieved a large range of applications in several areas of engineering. In many of these applications such materials are subjected to thermomechanical loading for which the thermal stress fields require particular attention. In these situations, the design of composite elements demands a previous thermal analysis aiming to evaluate the temperature field and its effects on the material behavior. To carry out this analysis, the material thermal conductivity is an essential property. The computation of the temperature field is an indispensable task for evaluation of the thermal stresses and, consequently, for the rational design of the composite systems.

The effective thermal conductivity of composites is a property that depends on many factors, such as, volume fractions and thermal conductivities of the constituent phases and microstructural characteristics, as distribution and geometrical shapes of the fibers [1, 2]. There are many analytical and numerical models proposed in the literature for evaluating effective thermal conductivity of composite materials. A lot of the existent analytical models consist in extensions of micromechanical model originally formulated for elastic homogenization of two-phase composites with random microstructure satisfying the statistical homogeneity condition [3–8]

Periodic composites constitute an important class of heterogeneous materials. In these materials, the fibers are periodically distributed into the matrix, so that their microstructures can be constructed by regularly replicated elementary block, named repeating unit cell (RUC) [9]. There are also a number of models proposed for thermal and mechanical homogenization of periodic composites. Many of these models use numerical methods, such as finite element method [10-13] and finite volume theory [14–16], in their formulations. Due to the microstructure periodicity, the Fourier series also have been employed for homogenization of periodic composites, as can be seen in [17–20] and [21, 22] for elastic and thermal problems, respectively.

This paper presents a theoretical investigation on the influences of the cross section geometry, contrast between thermal conductivities of the phases and volume fraction of the fibers on the effective thermal conductivity of unidirectional periodic fiber reinforced composites. The study is developed using a semi-analytical model expressed in terms of Fourier series and based on the thermal equivalent inclusion strategy [22]. This model incorporates an efficient procedure for determination of the transformation temperature gradient field related to the thermal equivalent inclusion strategy. The above mentioned influences are illustrated and discussed through several numerical examples. Results obtained by other homogenization procedures available in the literature are also presented to demonstrate the efficiency of the model used in the study.

2 Outline on thermal homogenization

Figure 1 illustrates a representative volume element (RVE) of a composite material, with volume D and boundary surface ∂D, subjected to a homogeneous temperature boundary condition given by

$$\boldsymbol{T^0}(\boldsymbol{x}) = \boldsymbol{G^0} \cdot \boldsymbol{x} \quad \text{for } \boldsymbol{x} \in \partial D \tag{1}$$

where $\boldsymbol{G^0} = \boldsymbol{\partial T^0}/\boldsymbol{\partial x}$ and $\boldsymbol{x}$ is the coordinate vector of points in D. The symbol $(\cdot)$ indicates scalar product of two vectors. The average values of the temperature and its average gradient vector taken on the RVE are defined respectively by

$$\bar{T}_D = \frac{1}{D}\int_D T(\boldsymbol{x})dD \tag{2}$$

$$\bar{\boldsymbol{G}}_D = \frac{1}{D}\int_D \boldsymbol{G}(\boldsymbol{x})dD \tag{3}$$

where $T(\boldsymbol{x})$ is the temperature field and $\boldsymbol{G}(\boldsymbol{x}) = \partial T(\boldsymbol{x})/\partial \boldsymbol{x}$ indicates the corresponding gradient vector. Applying the divergence theorem to Eq. (3), the following relation is obtained

$$\overline{\boldsymbol{G}}_D = \boldsymbol{G}^0 \tag{4}$$

meaning that the average temperature gradient vector over the entire RVE coincides with the temperature gradient applied on the RVE boundary surface, irrespective of the material microstructure. This last equation corresponds to the average temperature gradient theorem.

The microstructure of a periodic composite can be conceived as generated by repeating unit cells distributed regularly over the material domain, such as shown in Fig. 1. Here, $2a_1$, $2a_2$ and $2a_3$ indicate the RUC dimensions. In this case, the temperature field of a generic RUC can be expressed by using a two-scale representation, in the form

$$T(\boldsymbol{y}) = \boldsymbol{G}^0 \cdot \boldsymbol{x} + \tilde{T}(\boldsymbol{y}) \tag{5}$$

where the first term on the right side represents the macroscopic contribution and $\tilde{T}$ stands for the fluctuating temperature field. In Eq. (5), $\boldsymbol{y}$ and $\boldsymbol{x}$ indicate the local coordinates for the RUC scale and the global coordinates used in the RVE scale, respectively. Due to the material microstructure periodicity and RVE boundary condition homogeneity, $\tilde{T}(\boldsymbol{y})$ is a periodic function over the RUC domain.

From Eq. (5), the average temperature gradient over the RUC volume (V) can be obtained by

$$\overline{\boldsymbol{G}}_{\mathrm{V}} = \boldsymbol{G}^0 + \frac{1}{\mathrm{V}}\int_{\mathrm{V}} \widetilde{\boldsymbol{G}}\,(\boldsymbol{y})d\Omega \tag{6}$$

being $\widetilde{\boldsymbol{G}}(\boldsymbol{y}) = \partial\tilde{T}(\boldsymbol{y})/\partial\boldsymbol{y}$. Taking into account that $\widetilde{\boldsymbol{G}}(\boldsymbol{y})$ is also a periodic function over the RUC domain, the integral appearing in Eq. (6) is a null vector. Then,

$$\overline{\boldsymbol{G}}_{\mathrm{V}} = \boldsymbol{G}^0 \tag{7}$$

indicating that the average temperature gradient over the RUC coincides with the average temperature gradient over the RVE.

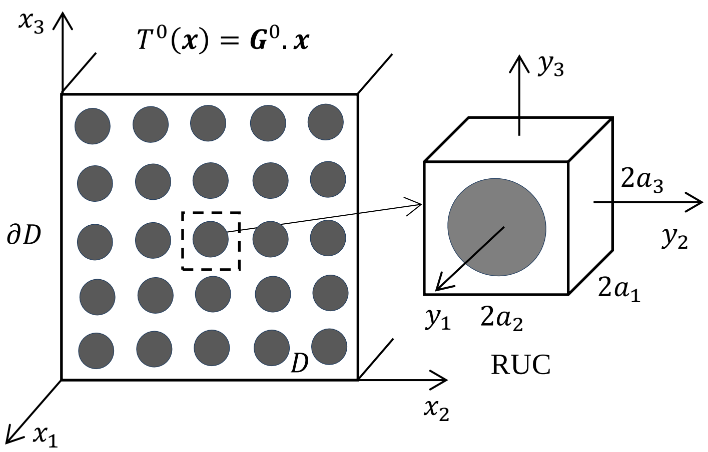

Figure 1. Periodic composite material and repeating unit cell (RUC)

3 Thermal equivalent inclusion problem

Figure 2(a) presents a typical RUC that constitutes a RVE of a periodic composite material subjected to a homogeneous temperature boundary condition. The RUC is composed by a matrix embedding a fiber with domain Ω. Under the mentioned boundary condition, the heat flux vector inside the fiber can be expressed by

$$\boldsymbol{q}(\boldsymbol{y}) = -\boldsymbol{k}_\Omega \boldsymbol{G}(\boldsymbol{y}) \quad \text{for } \boldsymbol{y} \in \Omega \tag{8}$$

being $\boldsymbol{k}_\Omega$ the thermal conductivity matrix of the fiber and $\boldsymbol{G}$ the local temperature gradient vector.

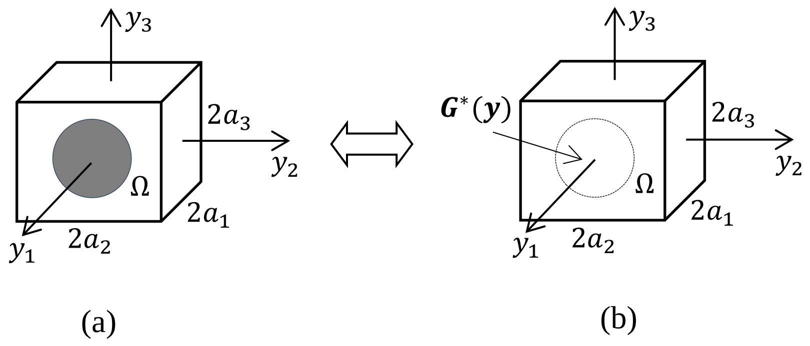

Figure 2. Equivalent inclusion thermal problem: (a) actual RUC and (b) homogeneous RUC

The equivalent inclusion thermal problem consists in to find a transformation temperature gradient $\boldsymbol{G}^*(\boldsymbol{y})$ that imposed over the domain Ω of the homogenized RUC, constituted only by the matrix material and under the same boundary condition, generates the same temperature and heat flux of the actual heterogeneous RUC (Fig. 2(b)). This problem can be defined by the consistency condition:

$$\boldsymbol{k}_\Omega\left[\boldsymbol{G}^0 + \widetilde{\boldsymbol{G}}(\boldsymbol{y})\right] = \boldsymbol{k}\left[\boldsymbol{G}^0 + \widetilde{\boldsymbol{G}}(\boldsymbol{y}) - \boldsymbol{G}^*(\boldsymbol{y})\right] \quad \text{for } \boldsymbol{y} \in \Omega \tag{9}$$

where $\boldsymbol{G}^*(\boldsymbol{y}) = \boldsymbol{0}$ for $\boldsymbol{y} \notin \Omega$ and $\boldsymbol{k}$ is the thermal conductivity matrix of the matrix material.

The periodic fluctuating temperature field $\tilde{T}(\boldsymbol{y})$ can be expanded in Fourier series in the form [22]

$$\tilde{T}(\boldsymbol{y}) = \sum_{\xi}^{\pm\infty} \hat{T}(\boldsymbol{\xi}) \exp(i\boldsymbol{\xi} \cdot \boldsymbol{y}) \tag{10}$$

with the components of $\boldsymbol{\xi}$ given by $\xi_k = \pi n_k / a_k$, (k=1,2,3), being $2a_k$ the RUC side dimensions (Fig. 2) and $n_k = 0, \pm 1, \pm 2, \ldots \pm \infty$. The series coefficients are defined as

$$\hat{T}(\boldsymbol{\xi}) = \frac{1}{\mathrm{V}} \int_{\mathrm{V}} \tilde{T}(\boldsymbol{y}) \exp(-i\boldsymbol{\xi} \cdot \boldsymbol{y}) d\Omega \tag{11}$$

Considering the definition of the fluctuating temperature gradient (Section 2), it follows the relation

$$\widetilde{\boldsymbol{G}}(\boldsymbol{y}) = \sum_{\xi}^{\pm\infty} \widehat{\boldsymbol{G}}(\boldsymbol{\xi}) \exp(i\boldsymbol{\xi} \cdot \boldsymbol{y}) \tag{12}$$

being $\widehat{\boldsymbol{G}}(\boldsymbol{\xi}) = i\,\hat{T}(\boldsymbol{\xi})\boldsymbol{\xi}$. Similarly, the periodic distribution of $\boldsymbol{G}^*(\boldsymbol{y})$ allows writing the Fourier series expansion

$$\boldsymbol{G}^*(\boldsymbol{y}) = \sum_{\xi}^{\pm\infty} \widehat{\boldsymbol{G}}^*(\boldsymbol{\xi}) \exp(i\boldsymbol{\xi} \cdot \boldsymbol{y}) \tag{13}$$

with

$$\widehat{\boldsymbol{G}}^*(\boldsymbol{\xi}) = \frac{1}{\mathrm{V}} \int_{\mathrm{V}} \boldsymbol{G}^*(\boldsymbol{y}) \exp(-i\boldsymbol{\xi} \cdot \boldsymbol{y})\, d\Omega \tag{14}$$

For the case of steady state heat conduction, without internal heat source, the heat flux vector satisfies the energy conservation law

$$\nabla\cdot\boldsymbol{q}(\boldsymbol{y}) = \nabla\cdot\boldsymbol{k}\left[\boldsymbol{G}^0 + \widetilde{\boldsymbol{G}}(\boldsymbol{y}) - \boldsymbol{G}^*(\boldsymbol{y})\right] = 0 \tag{15}$$

which, using (12) and (13), provides

$$\hat{T}(\boldsymbol{\xi}) = -i\,\frac{\boldsymbol{\xi}\cdot\boldsymbol{k}\widehat{\boldsymbol{G}}^*(\boldsymbol{\xi})}{\boldsymbol{\xi}\cdot\boldsymbol{k}\boldsymbol{\xi}} \quad \text{for} \quad \boldsymbol{\xi}\neq\boldsymbol{0} \tag{16}$$

Introducing (13) and (14) into (15), the following expression is obtained

$$\boldsymbol{G}^0 = -(\boldsymbol{k}_\Omega - \boldsymbol{k})^{-1}\boldsymbol{k}\boldsymbol{G}^*(\boldsymbol{y}) - \sum_{\boldsymbol{\xi}}^{\pm\infty}\frac{1}{\mathrm{V}}\boldsymbol{S}(\boldsymbol{\xi})\boldsymbol{k}\int_\Omega \boldsymbol{G}^*(\boldsymbol{y}')\exp(-i\boldsymbol{\xi}\cdot\boldsymbol{y}')\,d\,\Omega\exp(i\boldsymbol{\xi}\cdot\boldsymbol{y}) \tag{17}$$

where $\boldsymbol{S}(\boldsymbol{\xi}) = \boldsymbol{\xi}\boldsymbol{\xi}^t/(\boldsymbol{\xi}\cdot\boldsymbol{k}\boldsymbol{\xi})$. Discretizing the inclusion domain into subdomains or partitions Ω_j $(j = 1, 2, \ldots, N)$ and integrating the terms of Eq. (17) over each one of them, it follows that

$$f_j\boldsymbol{G}^0 = \sum_{k=1}^{N}\left[-(\boldsymbol{k}_\Omega - \boldsymbol{k})^{-1}\boldsymbol{k}\delta_{jk} - \frac{1}{\mathrm{V}\Omega_k}\sum_{\boldsymbol{\xi}}^{\pm\infty}\boldsymbol{S}(\boldsymbol{\xi})\boldsymbol{k}g_k(-\boldsymbol{\xi})g_j(\boldsymbol{\xi})\right]f_k\,\overline{\boldsymbol{G}}^*_{\Omega_k} \tag{18}$$

being $f_s = \Omega_s/\Omega$ $(s = 1, 2, \ldots, N)$ the subdomain volume fraction, $\boldsymbol{\xi}\neq\boldsymbol{0}$, $\delta_{jk} = 1$ for $j = k$, $\delta_{jk} = 0$ for $j \neq k$,

$$g_j(\boldsymbol{\xi}) = \int_{\Omega_j}\exp(i\boldsymbol{\xi}\cdot\boldsymbol{y})d\Omega_j \qquad\qquad g_k(-\boldsymbol{\xi}) = \int_{\Omega_k}\exp(-i\boldsymbol{\xi}\cdot\boldsymbol{y})d\Omega_k \tag{19}$$

and

$$\overline{\boldsymbol{G}}^*_{\Omega_k} = \frac{1}{\Omega_k}\int_{\Omega_k}\boldsymbol{G}^*(\boldsymbol{y})\,d\Omega_k \tag{20}$$

Finally, the solution of Eq. (18) for $\overline{\boldsymbol{G}}^*_{\Omega_k}$ can be written in the matrix form

$$\overline{\boldsymbol{\mathcal{G}}}^* = \boldsymbol{\mathcal{L}}^{-1}\boldsymbol{\mathfrak{J}}\boldsymbol{G}^0 \tag{21}$$

where $\overline{\boldsymbol{\mathcal{G}}}^* = \left\{\overline{\boldsymbol{G}}^*_{\Omega_1}\ \ \overline{\boldsymbol{G}}^*_{\Omega_2}\cdots\ \overline{\boldsymbol{G}}^*_{\Omega_N}\right\}^t_{(3N\times1)}$, $\boldsymbol{\mathfrak{J}} = [\boldsymbol{I}_3\ \ \boldsymbol{I}_3\ \cdots\ \boldsymbol{I}_3]^t_{(3N\times3)}$, $\boldsymbol{G}^0 = \{G^0_1\ \ G^0_2\ \ G^0_3\}^t_{(3\times1)}$ and

$$\boldsymbol{\mathcal{L}} = \begin{bmatrix} \boldsymbol{L}_{11} & \boldsymbol{L}_{12}\cdots\boldsymbol{L}_{1N} \\ \boldsymbol{L}_{21} & \boldsymbol{L}_{22}\cdots\boldsymbol{L}_{2N} \\ & \cdots\vdots \\ \boldsymbol{L}_{N1} & \boldsymbol{L}_{N2}\cdots\boldsymbol{L}_{NN} \end{bmatrix}_{(3N\times3N)}$$

with

$$\boldsymbol{L}_{jk} = -(\boldsymbol{k}_\Omega - \boldsymbol{k})^{-1}\boldsymbol{k}\delta_{jk} - \frac{1}{\mathrm{V}\Omega_j}\sum_{\boldsymbol{\xi}}^{\pm\infty}\boldsymbol{S}(\boldsymbol{\xi})\boldsymbol{k}g_k(-\boldsymbol{\xi})g_j(\boldsymbol{\xi})$$

and $\boldsymbol{I}_3$ indicating the (3x3) identity matrix. Then, the average value of $\boldsymbol{G}^*$ over the entire inclusion may be then evaluated in function of $\overline{\boldsymbol{G}}^*_{\Omega_k}$ $(k = 1, 2, \ldots, N)$ by

$$\overline{\boldsymbol{G}}^*_{\boldsymbol{\Omega}} = \sum_{s=1}^{N} f_s\overline{\boldsymbol{G}}^*_{\Omega_s} = \boldsymbol{\mathcal{F}}\boldsymbol{\mathcal{L}}^{-1}\boldsymbol{\mathfrak{J}}\boldsymbol{G}^0 \tag{22}$$

being $\boldsymbol{\mathcal{F}} = [f_1\boldsymbol{I}_3\ \ f_2\boldsymbol{I}_3\ \cdots f_N\boldsymbol{I}_3]_{(3\times3N)}$. More detail about this model can be seen in the reference [22].

4 Homogenized thermal conductivity of a unit cell

The effective thermal behavior of a periodic composite can be expressed in terms of volume-averaged quantities related to the RUC. The average heat flux is given by

$$\bar{\boldsymbol{q}}_V = \frac{1}{V}\int_V \boldsymbol{q}(\boldsymbol{y})dV = -\frac{1}{V}\int_V \boldsymbol{k}\left[\boldsymbol{G}^0 + \widetilde{\boldsymbol{G}}(\boldsymbol{y}) - \boldsymbol{G}^*(\boldsymbol{y})\right]dV \tag{23}$$

which, considering the periodicity of $\widetilde{\boldsymbol{G}}(\boldsymbol{y})$ over the RUC domain, becomes

$$\bar{\boldsymbol{q}}_V = -\boldsymbol{k}\left(\boldsymbol{G}^0 - f_\Omega \bar{\boldsymbol{G}}_{\boldsymbol{\Omega}}^*\right) \tag{24}$$

Introducing Eq. (22) into Eq. (24), the macroscopic heat conduction equation of the RUC can be written as

$$\bar{\boldsymbol{q}}_V = \boldsymbol{k}\left(\boldsymbol{I}_3 - f_\Omega \boldsymbol{\mathcal{F}}\boldsymbol{\mathcal{L}}^{-1}\boldsymbol{\mathfrak{J}}\right)\boldsymbol{G}^0 \tag{25}$$

Then, the effective thermal conductivity of the composite of the composite is given by the expression

$$\bar{\boldsymbol{K}} = \boldsymbol{k}\left(\boldsymbol{I}_3 - f_\Omega \boldsymbol{\mathcal{F}}\boldsymbol{\mathcal{L}}^{-1}\boldsymbol{\mathfrak{J}}\right) \tag{26}$$

5 Investigated examples

5.1 Influence of the fiber geometry

The objective of this example is to investigate the influence of the fiber cross section geometry on the effective thermal conductivity k_{eff} of periodic unidirectional long fiber composites. Three different composites reinforced by fibers with square, circular and octagonal cross sections are considered. It is assumed a ratio $k_\Omega/k_M = 666$, where k_Ω and k_M represent the thermal conductivities of the fiber and matrix, respectively. Figure 3 shows the fiber partitions used in the analyses. A total of 150 terms of the Fourier series have been used in this example.

Figure 4 illustrates the variation of the effective thermal conductivity of the composites in function of the fiber volume fraction f_Ω. It is observed that for fiber volume fraction smaller than 60% the effective thermal conductivity is practically the same for the three fiber geometries. On the other hand, for $f_\Omega > 60\%$ the geometry of the fiber has greater influence on the values of k_{eff}. For this latter range of fiber volume fraction, the curve k_{eff}/k_M for the composite reinforced with the circular cross section fibers is always above of those corresponding to the other fiber geometries. The values of k_{eff}/k_M for the composite with octagonal cross section fibers keep between those obtained for the other two fiber geometries in the investigated interval of f_Ω, being closer to the curve of the circular cross section. It is interesting to observe that the curves exhibit a high slope when f_Ω tends for the limit value $f_{\Omega\max}$ of each cross section geometry. This curve inclination depends on the ratio k_Ω/k_M.

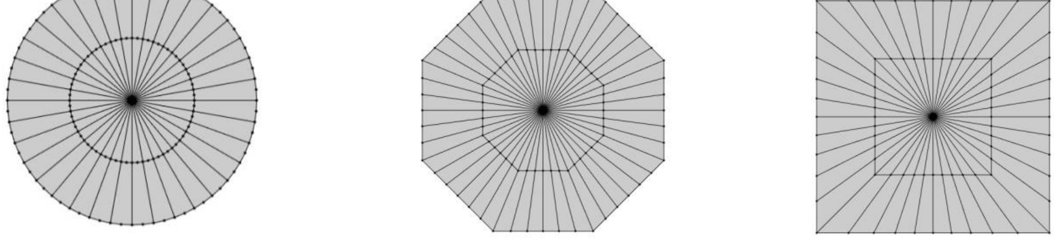

Circular fiber Octagon fiber Square fiber

Figure 4. Partitions of the fibers

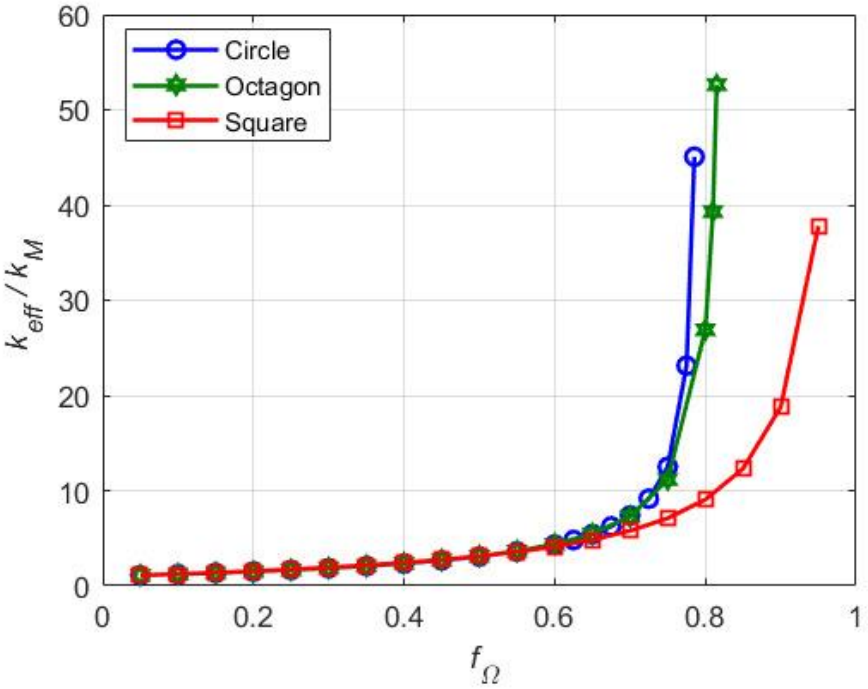

Figure 4. Effective thermal conductivities for composites with different fiber shapes

5.2 Influence of the contrast between phase thermal conductivities and fiber volume fraction

This section evaluates two-phase composites formed by a matrix reinforced with aligned continuous fibers. Both the composite constituents are considered isotropic in this study. The fibers are arranged in a square periodic array. The objective is to analyze the influences of the fiber volume fraction and mismatch between the thermal conductivities of the phases on the effective thermal conductivity of the composite, as well as the performance of the adopted homogenization model, when compared with FEM solutions. The three fiber partitions shown in Fig. 5 have been employed in the analyses.

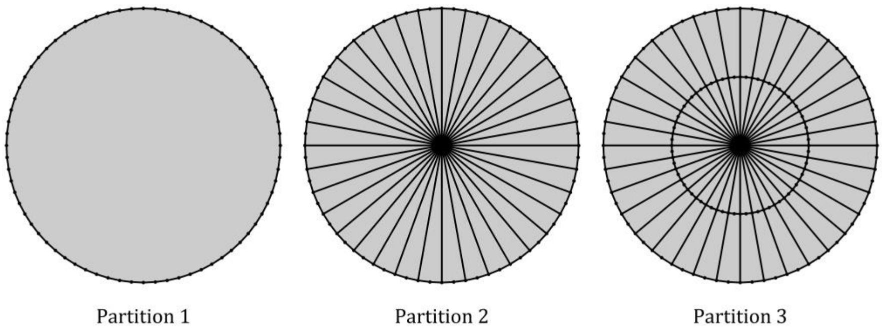

Figure 5. Partitions of the cylindrical fibers

Figures 6 and 7 illustrate the results obtained for k_{eff}/k_M in function of the fiber volume fraction f_Ω and ratio k_Ω/k_M, respectively, considering the partitions of Fig. 5. A total of 150 terms of the Fourier series were used in the analyses. The results of Fig. 6 have been generated for a ratio $k_\Omega/k_M = 666$, while those illustrated in Fig. 7 correspond to a fiber volume fraction of $f_\Omega = 0.60$. To comparison, the predictions obtained by Sihn and Roy [11], using finite element method (FEM), are also shown in Figs. 6 and 7. It is observed that the results provided by the present model for the partitions 2 and 3 are in excellent agreement with those obtained by the FEM. As already discussed in [22], the Partition 1 does not work well for cases of composites with large fiber volume fraction or large mismatch between the thermal conductivities of the matrix and fiber.

Considering the ratio k_Ω/k_M corresponding to Fig. 6, it is expected the monotonic increasing of the effective thermal conductivity for increasing values of f_Ω. Figure 7 also shows a continuous increasing of the effective thermal conductivity with the rise of the ratio k_Ω/k_M. In this case, the rate of increase is small for the range of low and high values of the mentioned ratio and more elevated for intermediate values ($0.1 < k_\Omega/k_M < 100$).

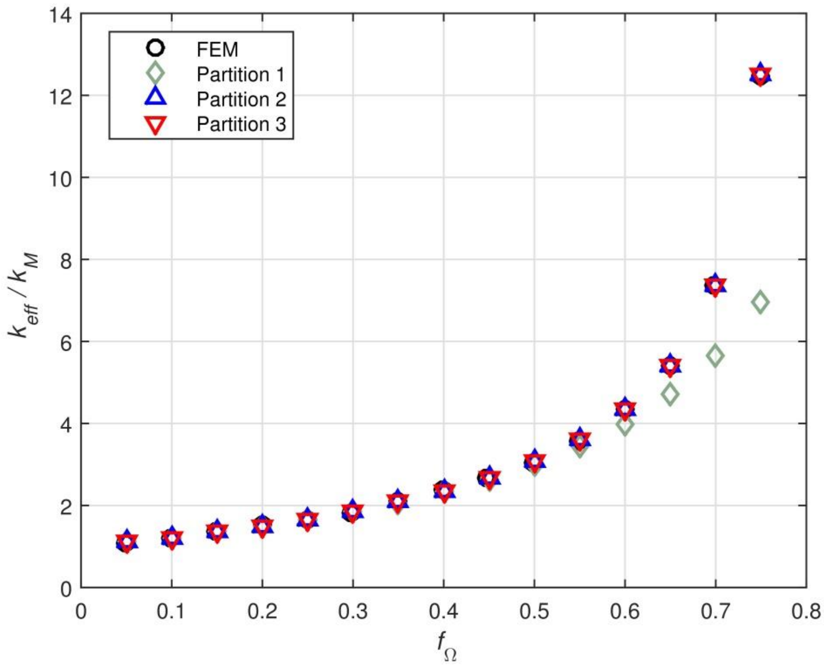

Figure 6. Effective thermal conductivity in function of the fiber volume fraction

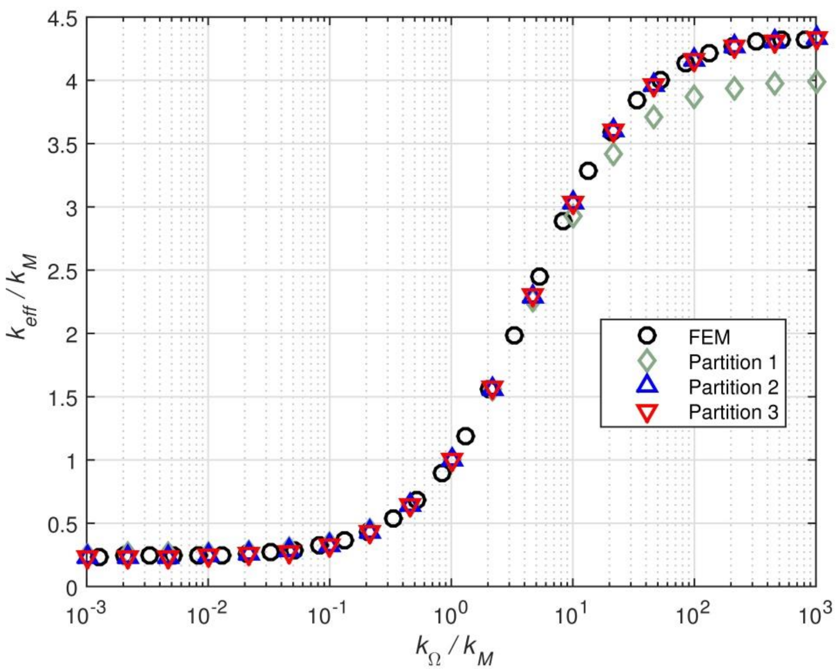

Figure 7. Effective thermal conductivity in function of the ratio k_Ω/k_M

6 Conclusions

This work presented a study about the influence of the fiber cross section geometry, fiber volume fraction and mismatch between the thermal conductivities of fiber and matrix on the effective thermal conductivity of two-phase periodic composites. The study has been developed using a micromechanical homogenization model based on the equivalent inclusion thermal problem, which uses Fourier series to represent the periodic variable fields. Composites reinforced with fibers of circular, octagon and square cross sections were analyzed. The results showed that the influence of the fiber geometry is more important for high fiber volume fractions. It was also observed that when the fiber domain is not discretized (Partition 1), the micromechanical model does not produce good solutions for composites with high fiber volume fractions and contrast between the thermal conductivities of the phase constituents. However, the model provided results in excellent agreement with finite element predictions for coarse partitions of the fiber domain, irrespective of the values of phase thermal conductivity ratio and inclusion volume fraction. Comparison with experimental results is interesting for additional validation of the adopted model.

Acknowledgements

The authors acknowledge the support provided by the Brazilian National Council for Scientific and Technological Development - CNPq to develop this work.

References

[1] T. Oppelt, T. Urbaneck, H. Böhme, B. Platzer. Numerical investigation of effective thermal conductivity for two-phase composites using a discrete model. *Applied Thermal Engineering*, vol. 115, pp. 1–8, 2017.

[2] J. - J. Gou, C. - L. Gong, L. - X. Gu, S. Li and W. - Q. Tao. Unit cells of composites with symmetric structures for the study of effective thermal properties. *Applied Thermal Engineering*, vol. 126, pp. 602–619, 2017.

[3] H. Hatta and M. Taya. Equivalent inclusion method for steady state heat conduction in composites. *International Journal of Engineering Science*, vol. 24, n. 7, pp. 1159–1172, 1986.

[4] Y. Benveniste. Effective thermal conductivity of composites with a thermal contact resistance between the constituents: nondilute case. *Journal of Applied Physics*, vol. 61, n. 8, pp. 2840–2843, 1987.

[5] Y. - M. Lee, R. - B. Yang and S. - S. Gau. A generalized self-consistent method for calculation of effective thermal conductivity of composites with interfacial contact conductance. *International Communications of Heat and Mass Transfer*, vol. 33, n. 2, pp. 142–150, 2006.

[6] N. Bonfoh, C. Dreistadt and H. Sabar. Micromechanical modeling of the anisotropic thermal conductivity of ellipsoidal inclusion-reinforced composite materials with weakly conducting interfaces. *International Journal of Heat and Mass Transfer*, vol. 108, pp. 1727–1739, 2017.

[7] N. Bonfoh and H. Sabar. Anisotropic thermal conductivity of composites with ellipsoidal inclusions and highly conducting interfaces. *International Journal of Heat and Mass Transfer*, vol. 118, pp. 498–509, 2018.

[8] J. Xiao, Y. Xu and F. Zhang. An analytical method for predicting the effective transverse thermal conductivity of nano coated fiber composites. *Composite Structures*, vol. 189, pp. 553–559, 2018.

[9] A. Drago and M. - J. Pindera. Micro-macromechanical analysis of heterogeneous materials: Macroscopically homogeneous vs periodic microstructures. *Composites Science and Technology*, vol. 67, n. 6, pp. 1243–1263, 2007.

[10] R. Rolfes and U. Hammerschmidt. Transverse thermal conductivity of CFRP laminates: A numerical and experimental validation of approximation formulae. *Composites Science and Technology*, vol. 54, n. 1, pp. 45–54, 1995.

[11] S. Sihn, A. K. Roy. Micromechanical analysis for transverse thermal conductivity of composites. *Journal of Composite Materials*, vol. 45, n. 11, pp. 1245–1255, 2011.
[12] J. C. Michel, H. Moulinec and P. Suquet. Effective properties of composite materials with periodic microstructure: a computational approach. *Computer Methods in Applied Mechanics and Engineering*, vol. 172, n. 1–4, pp. 109–143, 1999.
[13] J. Yvonnet, Q. - C. He and C. Toulemonde. Numerical modelling of the effective conductivities of composites with arbitrarily shaped inclusions and highly conducting interface. *Composites Science and Technology*, vol. 68, n. 13, pp. 2818–2825, 2008.
[14] M. A. A. Cavalcante, S. P. C. Marques and M. - J. Pindera. Parametric formulation of the finite-volume theory for functionally graded materials. Part I: Analysis. *Journal of Applied Mechanics*, vol. 74, n. 5, pp. 935–945, 2007.
[15] M. A. A. Cavalcante, M. - J. Pindera and H. Khatam. Finite-volume micromechanics of periodic materials: past, present and future. *Composites Part B*, vol. 43, n. 6, pp. 2521–2543, 2012.
[16] R. S. Escarpini Filho, S. P. C. Marques. A model for evaluation of effective thermal conductivity of periodic composites with poorly conducting interfaces. *Materials Research*, vol. 17, n. 5, pp. 1344–1355, 2014.
[17] S. Nemat-Nasser, T. Iwakuma and M. Hejazi. On composites with periodic structures. *Mechanics of Materials*, vol. 1, n. 3, pp. 239–267, 1982.
[18] T. Iwakuma and S. Nemat-Nasser. Composites with periodic microstructure. *Computers & Structures*, vol. 16, n. 1–4, pp. 13–19, 1983.
[19] R. Luciano and E. J. Barbero. Formulas for the stiffness of composites with periodic microstructure. *International Journal of Solids Structures*, vol. 31, n. 21, pp. 2933–2944, 1994.
[20] A. Caporale, L. Feo and R. Luciano. Eigenstrain and Fourier series for evaluation of elastic local fields and effective properties of periodic composites. *Composites Part B*, vol. 81, pp. 251–258, 2015.
[21] H. Le Quang, T. - L. Phan and G. Bonnet. Effective thermal conductivity of periodic composites with highly conducting imperfect interfaces. *International Journal of Thermal Sciences*, vol. 50, n. 8, pp. 1428–1444, 2011.
[22] E. N. Lages, S. P. C. Marques. A semi-analytical model for evaluation of effective thermal conductivity of composites with periodic microstructure. *Journal of the Brazilian Society of Mechanical Sciences and Engineering*, vol. 41:127, 2019.